Can we see the unseen? To better understand crack propagation a the origin of an avalanche and related physical principles

Charles-Élie Goujon, Alain Duclos, Cédric Perillat, Frédéric Pourraz

CAN WE SEE THE UNSEEN? TO BETTER UNDERSTAND CRACK PROPAGATION A THE ORIGIN OF AN AVALANCHE AND RELATED PHYSICAL PRINCIPLES

Charles-élie GOUJON[1*], Alain DUCLOS[2,3], Cédric PERILLAT[3], Frédéric POURRAZ[4]

[1] CEA,Grenoble, France,
[2] data-avalanche / [3]ALEA, Aussois, France
[4] Université Savoie Mont-Blanc, Annecy, France

ABSTRACT: Propagation Saw Tests (PST) are designed to evaluate the propensity for a snowpack layer to fracture and potentially lead to an avalanche. The PST offers valuable insights into the snowpack structural integrity, identifying weak layers that may fail under stress. By simulating conditions that can lead to slab avalanches, the PST assists in understanding the complex dynamics of snowpack stability. Currently, however, the assessment of PSTs relies heavily on human observation, and given the limitations of our perception, we might be overlooking some critical elements. These elements could provide a deeper understanding of the propagation of rupture and layer identification. Could there be aspects that our naked eye cannot detect? We conducted PSTs utilizing infrared imagers and event-based sensors to capture detailed imagery of the snowpack. This innovative approach enabled the examination of information beyond the visible spectrum with a SWIR imager and the detection of micro-movements within the snow using an event-based sensor. SWIR imaging offers a groundbreaking method for analyzing snowpack layers, revealing critical details invisible to the naked eye. By capturing sunlight reflected off the snow's surface, SWIR technology can differentiate between various layers, identify moisture content, and uncover hidden structural features. This capability enhances information on the snowpack, potentially helping us to better identify the weak layer and understand its behavior. Event-based sensors, with their capability to effectively achieve an equivalent of 10,000 frames per second, offer an advancement in understanding propagation during PST. These high-speed sensors capture dynamic changes within the snowpack as fractures develop and propagate, providing detailed insight into the rapid processes and interactions that precede avalanche initiation. Our experiments with SWIR imaging and event-based sensors have unveiled new features that could be followed to better understand rupture propagation. This innovative methodology introduces new parameters for snowpack and PST analysis. Following these new parameters could improve knowledge of the weak layer and the propagation of rupture.

KEYWORDS: SWIR, Event based sensor, propagation, high speed monitoring, propagation mechanics

1. INTRODUCTION

Avalanche forecasting is a critical aspect of mountain safety. Traditional methods, such as Column Test (CT), Extended Column Test (ECT) and Propagation Saw Test (PST) are widely used to evaluate the propensity for crack propagation within a weak layer, which can lead to potential slab avalanche triggering [Simenhois et al. (2009)]. Furthermore, these tests provide valuable data on fracture mechanics, improving the accuracy of avalanche forecasting and snowpack stability assessments. Although safety tools like ROMANsns process facilitates data recording and treatment [Pourraz et al. (2023a)], these methods rely heavily on human observation, which is inherently limited by perceptual and interpretive biases. Human observers may miss subtle but significant indicators of instability, leading to incomplete or inaccurate assessments of avalanche risk. To overcome human limitations, there is a growing interest in leveraging advanced sensing technologies to enhance understanding, precision and reliability of snowpack evaluations [Bergfeld et al. (2021), Bergfeld et al. (2022)].

This study explores the application of Short-Wave InfraRed (SWIR) imaging and event-based sensors in the context of PST and ECT tests. SWIR imaging offers a different approach to analyse snowpack layers by capturing details beyond the visible spectrum, such as variations in moisture content and subtle structural features that are invisible to the naked eye [Hammonds et al. (2023)]. Meanwhile, event-based sensors provide a dynamic method for monitoring the rapid propagation of fractures, recording high-speed changes in the snowpack at rates equivalent to 10,000 frames per second.

These new sensors, provided by PROPHESEE and LYNRED, are lightweight and can be easily used in real mountain conditions. By integrating

* *Corresponding author address:*
Goujon Charles-élie, CEA-Grenoble, 17 Avenue des Martyrs, 38400 Grenoble;
tel: +33 438786261
email: charleselie.goujon@cea.fr

these technologies into traditional snow stability field tests, we aim to observe new parameters and open doors that might enhance the understanding of fracture dynamics and propagation phenomenon.

This collaborative work between the Innovation team at CEA-Grenoble, data-avalanche, ALEA, and University Savoie Mont Blanc is an exploratory approach to observe new parameters and determine if they could improve our knowledge and understanding. This paper presents the methodology, results, and implications of utilizing these advanced sensing techniques.

2. METHODE

2.1 Field Experiment

ROMANsns (Réseau d'Observations et de Mesures Avalanches et Neige en secteur non sécurisé) is a collaborative network focused on avalanche and snow observations in unsecured areas. Observers use specific tests and mobile tools to gather data [Pourraz et al. (2023a)], which are then utilized by mountain professionals and road safety managers in their decision process [Pourraz et al. (2023b), Pourraz et al. (2023c)]. The ROMANsns protocol is based on a combination of three tests: CT, ECT and PST [Pourraz et al. (2023a)]. It aims to study snowpack behavior, particularly crack propagation in buried weak layers, in order to improve avalanche danger assessment. This protocol has been developed with the help of a smartphone application that guides the observer to ensure measurement homogeneity. It also facilitates result recording, regardless of weather conditions, and enables real-time sharing [Pourraz et al. (2023c)].

We conducted two test sessions in the French Alps. The first one was on April 27, 2023, in Bonneval/Arc - Pointe d'Andagne sector, and the second one was on April 8, 2024, in Val-Cenis - Pointe de Cugne sector (see Figure 1).

To perform our experiments, we placed imagers in front of the snow profile while conducting CT, ECT, and PST tests (see Figure 2).

By performing tests under different winter conditions, both of which involving the presence of one or more weak layers, we aim to compare our observations and potentially discover new parameters for understanding slab avalanche triggering process. To make our system portable, we used the setup shown opposite (see Figure 3).

Figure 1: Encircled in red, the Pointe de Cugne sector where the field test in real condition took place thanks to lightweight and compact sensors.

Figure 2: Event sensor placed in front of the snow beam during session 2.

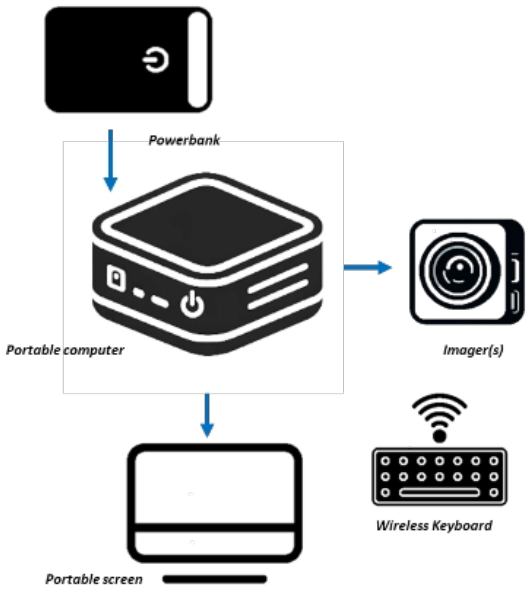

Figure 3: Experiment portable setup.

For our subsequent experiments, we used two different sensors. The EVK4-HD from Prophesee is an ultra-light and compact event-based camera featuring the Sony IMX636 sensor. It is designed for high-speed, low-latency vision applications, offering a resolution of 1280x720 pixels and a dynamic range greater than 120 dB. The Lynred SNAKE SW is a SWIR (Short-Wave Infrared) sensor designed for high performance in demanding environments. It features a compact design, a resolution of 640x512 pixels, and sensitivity across the SWIR spectrum (900nm-1700nm), making it ideal for applications in defense, surveillance, and industrial inspection.

To use and test these imagers, we utilized the ADDVISIA platform (see Figure 4), developed by CEA in collaboration with ST, LYNRED, and Prophesee. ADDVISIA is the result of an initiative by IRT Nanoelec. The ADDVISIA Technology Dissemination Hub leads a community of interest focused on multimodal and multispectral imaging to explore the full potential of combined imagers and identify new applications.

Figure 4: ADDVISIA multimodal platform.

The ADDVISIA multimodal platform covers a broad spectrum. In our case, we will focus on the visible spectrum for the PROPHESEE sensor and the SWIR spectrum for the Lynred SWIR sensor. The event sensor will help us overcome human limitations by capturing very fast events, while the SWIR sensor will help us surpass the limitations of the human eye, which is restricted to the visible spectrum.

2.2 *What can we see beyond the visible spectrum?*

The SWIR spectrum ranges from 0.9 to 2.5 microns, positioned between the visible and mid-wave infrared regions. Unlike the visible spectrum, which is seen by the human eye, SWIR can penetrate fog, dust, and other obscurants while providing high contrast and clarity. SWIR is widely used in various applications, including industrial inspection, surveillance, and medical imaging, due to its ability to reveal details invisible to both visible and other infrared wavelengths.

SWIR sensors have been used for years in satellite applications to collect data beyond the visible spectrum. Reid et al. (2014) used SWIR wavelengths to classify ice (see Figure 5.a), while C. Schlundt et al. (2011) used SWIR to determine snow grain size (see Figure 5.b).

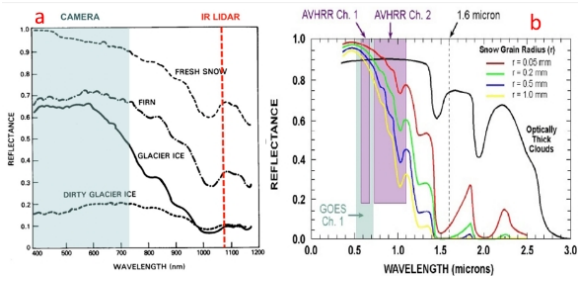

Figure 5: a: Multispectral Ice Classification from Reid et al. (2014). b: Reflectance spectrum from Schlundt et al. (2011).

These works show that within the SWIR range, there are parameters that can help differentiate snow types. Recently, with a greater focus on avalanche risks, Horton et al. (2017) investigated the spectral reflectance of surface hoar crystals using a field spectrometer (see Figure 6), and Hammonds et al. (2023) demonstrated that with multispectral imagers, they could detect liquid water in snow.

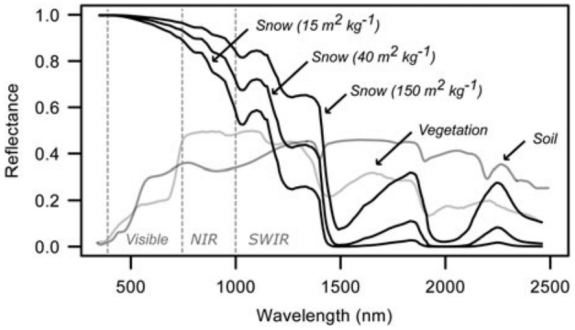

Figure 6: Spectral hemispherical reflectance (Horton et al. (2017).

Some of these works use spectrometers. Using a SWIR imager can provide both spectral and spatial information, allowing us to compare different types of layers.

2.3 *What can we see beyond the speed of the human eye?*

Event-based sensors detect changes in a scene by capturing pixel-level brightness variations, allowing for high-speed and low-latency imaging.

Unlike traditional frame-based sensors, they only record significant changes, reducing data redundancy and power consumption. These sensors are ideal for applications requiring fast, efficient processing, such as robotics, autonomous vehicles, and surveillance. Event sensors are a relatively new technology, making them not yet easily accessible and not widely used. Unlike SWIR imaging, there is no previous work on snow with event sensors.

3. RESULTS AND DISCUSSION

3.1 SWIR imaging

During our first session in 2023, we captured this SWIR image (see Figure 7) using an optical filter of 900-1375 nm to focus on the highest difference in spectral response.

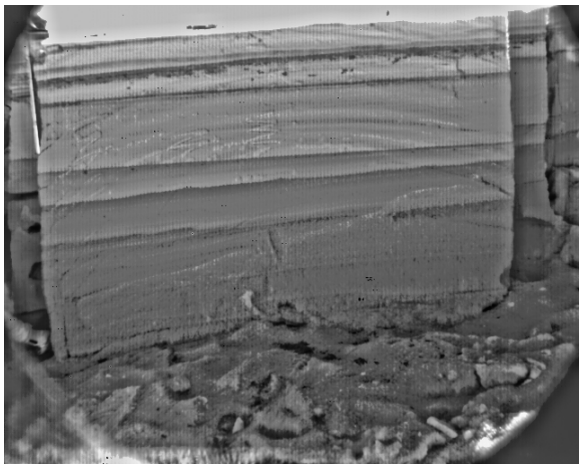

Figure 7: SWIR imaging of snow profile column.

What we can see is that SWIR imaging enhances snow stratigraphy by high-revealing the different layer interfaces. To emphasize the contrast, we are using image post-processing techniques (contrast enhancement algorithms) to better show these different layers. The curved lines we see are due to the wire used to cut the snow in order to isolate the snow test column. Comparing these images with the ROMANsns profile obviously highlights similarities (see Figure 8): the “classical” analysis leaded first remains an approved technique.

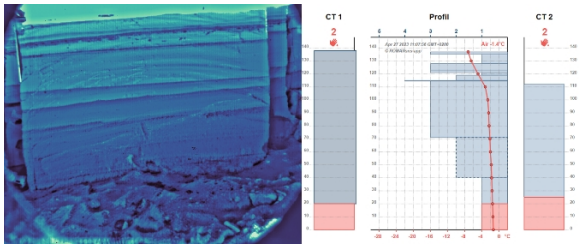

Figure 8: SWIR image and ROMANsns results from 2023 session.

Nevertheless, some details were invisible to the naked eye, so that SWIR technique could help us to better understand and have an accurate interpretation of the real snow profile.

To confirm this initial observation, we repeated the same test during our second session in 2024, using new methods to collect and post-process the data.

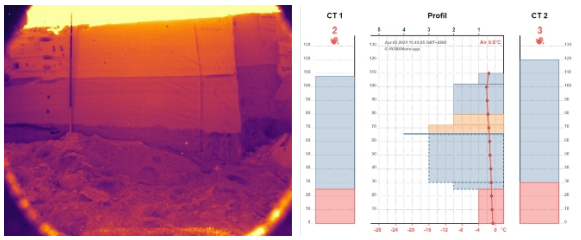

Figure 9: SWIR image and ROMANsns results from 2024 session.

In our 2024 session, the snowpack was different, as shown by the ROMANsns profile and the SWIR image (see Figure 9), indicating that SWIR data are consistent with the ROMANsns results. The visible image of this snowpack (see Figure 2) shows the sand layer indicated in the ROMANsns results. In the SWIR image, we can clearly see the three main layers of our snowpack. The bottom darker area represents the depth hoar zone of our snowpack, depicted in red in the ROMANsns results, as expected based on previous studies (see Figures 5 and 6).

We can see darker areas in our snowpack that may illustrate different physical properties of the snow (water content, type of grains, size, etc.). The complexity lies in the fact that it can be a mix of all these properties.

Thanks to SWIR images, we have been able to reconstruct the snowpack's "snow history" by visualizing the snow layers.

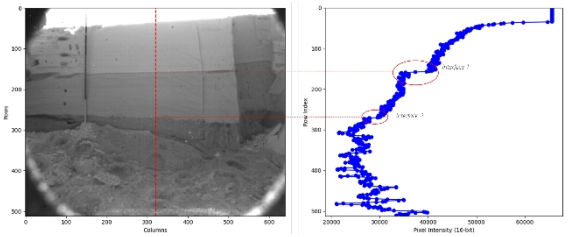

Figure 10: SWIR image (2024) and profile analysis.

By performing a profile analysis along a line (see Figure 10), we can see our two main interfaces. The gradients of these two interfaces are different, as are their levels. Perhaps gradient and level in SWIR are two new parameters to follow.

SWIR wavelengths can definitely provide more information than our naked eye. However, more

tests should be performed to determine which parameters should be followed and what information we can extract from them.

3.2 Event-based sensor

During our first session in 2023, we recorded event data while conducting PSTs. From this data, we can extract events and recreate frames by accumulating events over a certain period. The accumulation process is explained as follows:

$$for\ each\ event:$$

$$e=(x,y,t_e,p)$$

$$within\ the\ time\ window\ [t,t+\Delta t]:$$

$$F_t(x,y) \leftarrow F_t(x,y)+p$$

Where x,y are the pixel position, t_e the time-stamp and p the polarity of the event.

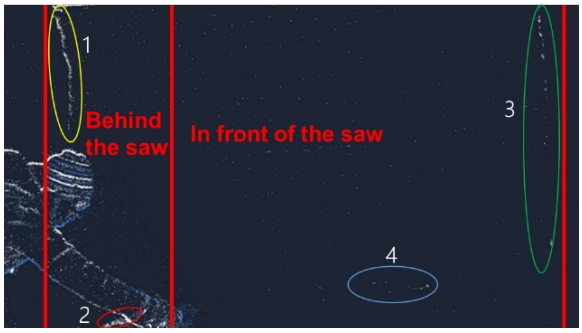

Figure 11: Image re-constructed from event data, with the different moving-area.

We used a sufficient accumulation time to cover the start and the entire propagation of the crack to construct the image (see Figure 11). To better understand the rest of our work, we define two areas: "behind the saw", the area where the saw has already damaged the weak layer, and "in front of the saw", the area where the saw has not yet damaged the weak layer. The question is, with this type of sensor, can we better understand how the grains "in front of the saw" know they can begin to disintegrate spontaneously, solely under the driving force exerted by the weight of the superior slab.

With the previously reconstructed image (see Figure 11), we can see four areas of interest. To analyze these different areas over time, we reconstructed images with a smaller accumulation time and created a 3D representation to integrate time variation (see Figure 12).

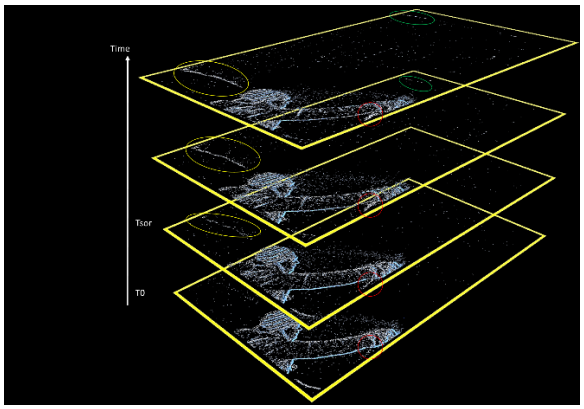

Figure 12: 3D time frame representation.

In the red area, we can see movement behind the saw. At the same time, in the second image from T0, we can see movement in the top left side (yellow area), indicating a bending of the slab. Finally, in the green area, in front of the saw on the right side of the snow profile, we can see movements indicating crack propagation from left to right.

T_{SOR} indicate the time when the Start Of Rupture occurs, which is when the superior slab bends due to the involved strains of the saw cut, but without propagation at this time. These observations show that there is a mechanical phenomenon behind the saw, generating strains and mechanical faults that can propagate through the rest of the snow beam. In discussions with Pr. François Louchet, we are questioning whether it follows the theoretical schema (see Figure 13).

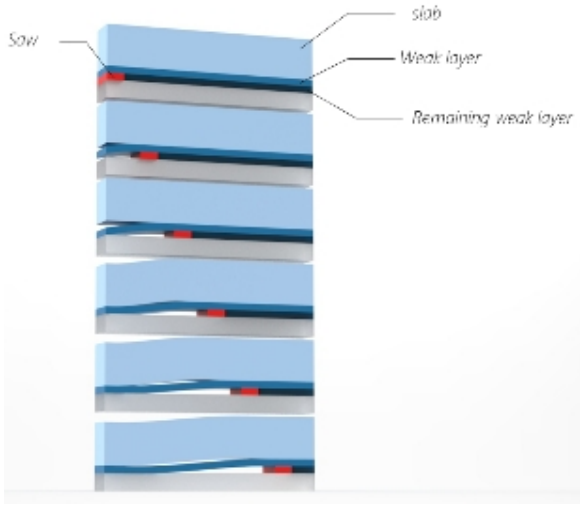

Figure 13: hypothesis of crack generation schema, with the generated shear strains appearing at the interfaces, due to the different stiffness of the involved slabs, and which could generate the crack propagation.

During the second session in 2024, we decided to delve deeper into our event data analysis. We used the sensor's parameters to collect even small changes in contrast, and applied a low-pass filter to clean our data. To represent our data, we follow the following expressions.

$$for\ each\ event:$$

$$t < E_{temporal}(x, y, v, t) < t + \Delta T$$

$$construct\ the\ entire\ image$$

$$I_T[x, y] = ¿$$

$$\int_{t=0}^{t=\Delta T} E_{temporal}(x, y, true, 0 < t < T_{base})\, dt$$

$$I_T[x, y]: Temporal\ image$$

$$T_{base}: Base\ time\ accumulate\ events$$

We decided to use $T_{base} = 400\,ms$, $\Delta T = 20\,ms$ Our complete period of analysis is 2 seconds. We have 5 frames to represent the entire period, and we colorize our frames based on the events' timestamps. The color scale is represented on the right of each frame.

During our test, using CTs, we identified two weak layers at different depths. We conducted a PST in the higher weak layer and observed a collapse and propagation without sliding (see Figure 14).

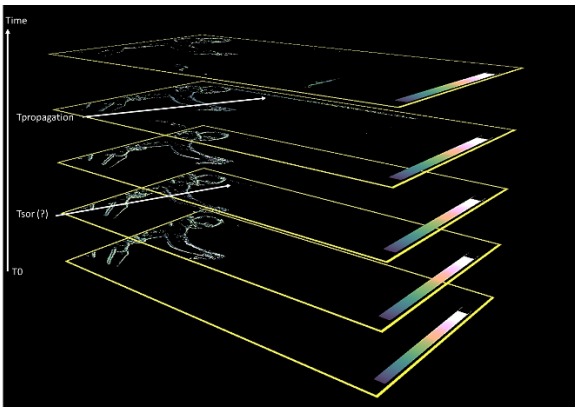

Figure 14: PST 1.

Some movements identified in the 2nd frame might indicate the start of rupture, but the top left is hidden, so it is not as clear as our first test.

After performing this first PST, we decided to conduct another PST in the lower weak layer identified within the snowpack (see Figure 15).

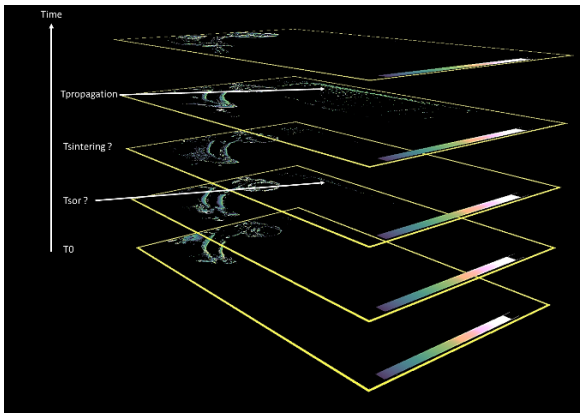

Figure 15: Slices from PST 2.

On the 2nd frame, we can see a bending of the slab in the top left corner, which can be identified as the start of rupture. Unlike our first observation in 2023, we see movements at the top of the snow beam further than the saw. In the next frame, there is less movement, which could indicate either an incomplete propagation or a sintering effect, which is something that should be investigated. Finally, in the 4th frame, we see the propagation, characterized by the collapse of the slab.

A complete visualisation of those two successive PSTs is shown in one graph in Figure 16.

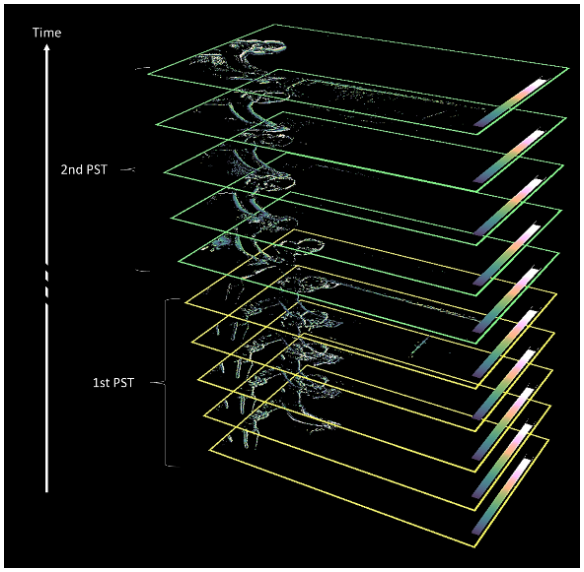

Figure 16: Slices from PST 1 & 2.

It's interesting to observe that the temporal delay between each similar frame from the first and the second PST remains the same, indicating the same kinetic of propagation in these two different weak layers. Nevertheless, further investigations should be performed in order to refine these observations and conduct reliable crack speed measurements.

3.3 *Multiple propagation phenomenon*

Furthermore, it's worth highlighting that while conducting tests during the first session, we encountered a specific phenomenon. During a PST, an initial propagation occurred without causing the isolated snow test column to slide. A second PST in the same weak layer was then performed, and during this test, a second propagation occurred, causing the entire snow test column to slide. This is illustrated in the following figure (see Figure 17).

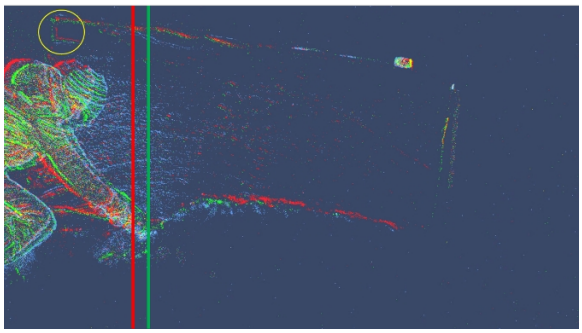

Figure 17: representation of two propagation in the same weak layer (first one in red and second one in green).

We have accumulated all the events from the first and second propagations, with the first one in red and the second one in green. Both propagations follow the same weak layer but with slight variations. The second propagation is lower, as a first collapse has already occurred due to the previous propagation, and it happens a bit farther along, as indicated by the hand being slightly further away (represented by the two lines). This illustrates that there are conditions where a weak layer can be potentially active multiple times without causing sliding, as it supposes to happen when "whumpf" occurs without slab release. To go further in the comprehension of this phenomenon, during the second session in 2024, we decided to perform a PST from the mountain side to gain a different perspective without mask effect by the operator. We isolated the snowpack with enough space to conduct the PST from behind (see Figure 18).

In this test, we performed 6 successive PSTs in the same weak layer before the complete sliding of our snow beam.

To visualize this, we decided to plot the 6 propagations in the same image (see Figure 19). The color scale from bottom to top illustrates the propagation number, with the first propagation at the bottom of the scale and the last one at the top. For each propagation, we used a 1-second timeline centered on the propagation event.

Figure 18: Mountain side PST.

Figure 19: Multiple propagation representation.

Each PST was positive, i.e. the bending of the slab implies the crack propagation into the weak layer, which is successively followed by the slab collapse. We can see that the snow beam moved after each propagation, finally leading to the complete slide of the slab, probably because of the enhancement of its global angle due to saw cut (the slope angle measured initially was 26°). This raises further questions: is the slab lying in a crushed weak layer which remains active several successive times due to a new stable state or a sintering phenomenon like that can appear in the shovel (see Figure 20)? More tests should be performed to refine this observation.

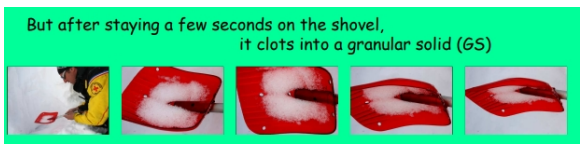

Figure 20: Shovel test by Duclos et al. (2009).

4. CONCLUSION AND PERSPECTIVES

The aim of this study was to use new sensors to overcome the limitations of human perception by capturing information beyond the visible spectrum and faster than the human eye. By using these new sensors, we questioned whether there are new parameters to follow.

We conducted tests in two separate sessions to compare our data across different winters, allowing us to refine our observations. Thanks to SWIR imagers, we can see beyond visible information and have been able to image the snow history of a snowpack, similar to tree rings. Analyzing this snowpack with a profile analysis revealed two worthwhile parameters to follow (gradient and level), which could help improve our knowledge.

With event sensors, we can capture very high-speed phenomena with a camera no bigger than an action camera. This opens up a field of analysis for high-speed events, such as crack propagation and slab collapse in unsecured areas. Using this type of sensor, it should be possible to approach crack speed measurements without using targets or accelerometers.

To conclude, following CTs and PSTs with this innovative approach could improve our knowledge, with new parameters highlighting potentially highly active weak layers. Indeed, four days after our second test, near where we conducted them, a large avalanche occurred during an ACP (Avalanche Control Process) (see Figure 21).

Figure 21: Haute-Maurienne Avalanche dated 09/04/2024 from data-avalanche database.

5. ACKNOWLEDGEMENT

This study was supported by IRT NANOELEC that is driving the ADDVISIA program.

This work is from the collaboration between CEA-Grenoble, data-avalanche, ALEA, University Savoie Mont Blanc, and the expertise from Pr. François LOUCHET.

6. REFERENCES

Bergfeld, B., van Herwijnen, A., Bobillier, G., Larose, E., Moreau, L., Trottet, B., Gaume, J., Cathomen, J., Dual, J. and Schweizer, J.: Crack propagation speeds in weak snowpack layers, Journal of Glaciology, 68(269), 557-570, 2022.

Bergfeld, B., van Herwijnen, A., Reuter, B., Bobillier, G., Dual, J. and Schweizer, J.: Dynamic crack propagation in weak snowpack layers: insights from high-resolution, high-speed photography, The Cryosphere, 15, 3539–3553, 2021. https://doi.org/10.5194/tc-15-3539-2021, 2021.

Duclos,A., Caffo,S., Bouissou M., Blackford J., Louchet F. and Heierli J.: Granular phase transition in depth Hoar and facets: a new approach to snowpack failure?, in: Proceedings of the International Snow Science Workshop, Davos, Switzerland, 27 September – 2 October 2009.

Hammonds, K., Donahue, C. and Skiles, M.C. : Detecting liquid water in snow and retrieving snow properties with hyperspectral imaging and upward looking radar: a new era in snowpit characterization and remote sensing, in: Proceedings of the International Snow Science Workshop, Bend, USA, 8-13 October 2023, 1058-1062, 2023.

Horton S. and Jamieson B.: Spectral measurements of surface hoar crystals, Journal of Glaciology, 63(239), 477-486. https://doi:10.1017/jog.2017.6, 2017.

Pourraz, F., Duclos, A. and Louchet, F.: An innovative protocol for conducting and exploiting snow tests: the outcome of a reliable field experiments and the development of digital tools on smartphone, in: Proceedings of the International Snow Science Workshop, Bend, USA, 8-13 October 2023, 295-302, 2023.

Pourraz, F., Duclos, A. and Coubat, G.: Cristal: a framework and tools for responsible decision-making, in: Proceedings of the International Snow Science Workshop, Bend, USA, 8-13 October 2023, 373-379, 2023.

Pourraz, F., Vallée, T., Lorentz, C. and Duclos, A.: Synthesis: the online tool providing easy access and systematic cross-checking of all useful information for avalanche danger assessment, in: Proceedings of the International Snow Science Workshop, Bend, USA, 8-13 October 2023, 937-943, 2023.

Reid, T., Walter, T., Enge, P. and Fowler, A.: Crowdsourcing arctic navigation using multispectral ice classification & GNSS, in: Proceedings of the 27th International Technical Meeting of the Satellite Division of The Institute of Navigation, Tampa, Florida, September 2014, 707-721, 2014.

Schlundt, C., Kokhanovsky, A. A., von Hoyningen-Huene, W., Dinter, T., Istomina, L. and Burrows, J. P.: Synergetic cloud fraction determination for SCIAMACHY using MERIS, Atmospheric Measurement Techniques, 4-2, 319-337, 2011. https://doi.org/10.5194/amt-4-319-2011, 2011.

Simenhois, R. and Birkeland, K.: The Extended Column Test: test effectiveness, spatial variability, and comparison with the Propagation Saw Test, Cold Regions Science and Technology, 59, 210-216, 2009.